

## Mechanical behavior of water filled C60

K. Min, A. Barati Farimani, and N. R. Aluru<sup>a)</sup>

*Department of Mechanical Science and Engineering, Beckman Institute for Advanced Science and Technology, University of Illinois at Urbana-Champaign, Urbana, Illinois 61802, USA*

(Received 18 October 2013; accepted 11 December 2013; published online 30 December 2013)

We present the mechanical properties of  $\text{H}_2\text{O}(n)@\text{C60}$  under hydrostatic strain and a point load using Density Functional Theory. In each case, we performed mechanical tests under both tension and compression. The bulk modulus and elastic modulus increase as the number of water molecules increases. For fracture behavior, two mechanisms are observed: First, under compression, due to the interaction and bond formation between water and C60, structures with more water molecules begin to exhibit fracture at a lower strain. Second, under tension, fracture is initiated from the bond dissociation of C-C bonds on the C60 surface. © 2013 AIP Publishing LLC. [<http://dx.doi.org/10.1063/1.4858486>]

The encapsulation of a single water molecule inside C60 opens up new opportunities for fabrication of novel electronic systems, such as memories, molecular motors, and mechanical nano-resonators.<sup>1</sup> Similarly, storage of hydrogen, nitrogen, and other molecules becomes feasible inside nanometer systems like C60.<sup>2,3</sup> Molecular scale confinement can alter the properties of caged molecules. For example, a single water molecule in C60 has dipole moment equal to  $1/4$  of its bulk value.<sup>4</sup> The vibrational frequencies and rotational motion of a single water molecule are affected by the imprisonment because the hydrogen bonding to the other water molecules is restricted by the cage.<sup>5</sup> Graphitic materials, such as carbon nanotubes, graphene, and buckyball, have been shown to have excellent mechanical properties.<sup>6–10</sup> C60, because of its spherical nature, can enable development of strong composite materials. It has been shown that C60 can enhance the mechanical properties when incorporated inside polymers.<sup>11,12</sup> On the other hand, insertion of other molecules inside C60 can enhance the mechanical properties of C60. Shen showed that putting Si or Ge inside C60 can increase the mechanical response under compression using Molecular Dynamics (MD) simulations.<sup>13</sup> However, the mechanical behavior of water filled buckyball and the interaction between water and the buckyball surface, which can significantly affect the mechanical response under various loading conditions, have not been studied. Moreover, the origin of mechanical failure due to the presence of water molecules inside C60 is still unknown. The studies performed here on water filled C60 can provide good insights into the application of water filled C60 as agents in composite materials.

In this Letter, we investigate the effect of water encapsulation on the mechanical properties of C60. We inserted water molecules in C60, and simulated these systems ( $\text{H}_2\text{O}(n)@\text{C60}$ ,  $n = 1, 3, 4$ , with  $n$  being the number of water molecules) using Density Functional Theory (DFT). Two different types of loading, a point load and a hydrostatic strain, are considered. For each type of loading, both compression and tension tests were performed to obtain the

mechanical strength of  $\text{H}_2\text{O}(n)@\text{C60}$ . Due to the spherical nature of C60, interesting mechanical responses were captured under various loading conditions. Bond-dissociation of buckyball and bond-formation between water and C60 are shown to play an important role for the fracture behavior.

To understand the physical and mechanical nature of C60 filled with water, DFT calculations using SIESTA were performed.<sup>14</sup> DFT is widely used because it can accurately capture the mechanical and electronic properties of nanomaterials under various conditions.<sup>15–19</sup> For parameterization of the exchange-correlation functional, generalized gradient approximation (GGA) with revised Perdew-Burke-Ernzerhof (RPBE) is used.<sup>20,21</sup> The core electrons are replaced by the norm-conserving pseudo-potentials.<sup>22</sup> For the basis set, double zeta basis plus polarization (DZP) numerical atomic orbital is used. For the k-point mesh generation, the  $\Gamma$  point is used. To remove any artificial effect of interaction between  $\text{H}_2\text{O}(n)@\text{C60}$  in the periodic simulation box, a vacuum region of around 15 Å is used in all directions. Structural relaxation is achieved until the maximum residual force of the system is reached, which is less than 0.03 eV/Å.

First, mechanical properties under hydrostatic strain are investigated. Hydrostatic pressure ( $P$ ), and bulk modulus ( $B$ ) are defined as  $P = |dE/dV|$ , and  $B = V_0(\partial^2 E/\partial V^2)$ , where  $E$  is the total energy and  $V$  is the volume of  $\text{H}_2\text{O}(n)@\text{C60}$ . The hydrostatic (volumetric) strain ( $\varepsilon_v$ ) is defined as  $\varepsilon_v = (V_s - V_0)/V_0$ , where  $V_0$  is the initial volume and  $V_s$  is the deformed volume. The hydrostatic strain is applied as follows: (a) The structure is relaxed for calculation of the initial total energy of the system. (b) Either tensile or compressive hydrostatic strain is applied to  $\text{H}_2\text{O}(n)@\text{C60}$ . (c) The strained C60 atoms are fixed, and water molecules inside C60 are relaxed. (d) The total energy of the deformed system is computed. (e) Steps (b)–(d) are repeated until the fracture of the system.

Mechanical properties under a point load are also considered, and similar procedure, as introduced above, is used. Elastic modulus ( $E_p$ ) and stress ( $\sigma$ ) are defined as  $E_p = (1/V_0)(\partial^2 U/\partial \varepsilon^2)$  and  $\sigma = \partial U/\partial \varepsilon$ ; these are obtained from the variation of the strain energy ( $U$ ) with applied strain ( $\varepsilon$ ), which is defined as  $\varepsilon = (d_s - d_0)/d_0$ , where  $d_0$  is the initial distance of two outermost carbon atoms in  $\text{H}_2\text{O}(n)@\text{C60}$ ,

<sup>a)</sup> Author to whom correspondence should be addressed. Electronic mail: [aluru@illinois.edu](mailto:aluru@illinois.edu)

TABLE I. DFT results for (2nd column) average C-C bond-length (double and single bonds), (3rd column) total energy of the initially relaxed system, and (4th column) interaction energy between water molecules and C60. DFT (5th column) and MD (6th column) results for internal pressure due to water molecules.

Structure	C-C Bond-length (Å) (double, single)	Total energy (eV)	Interaction energy (kcal/mol)	Internal pressure (GPa)	
				DFT	MD
C60	1.407,1.456	-9278.08	n/a	n/a	n/a
H <sub>2</sub> O(1)@C60	1.411,1.457	-9745.77	-17.34	0.01782	0.0049 (±0.0012)
H <sub>2</sub> O(3)@C60	1.418,1.466	-10675.85	56.34	12.9883	3.97 (±0.45)
H <sub>2</sub> O(4)@C60	1.424,1.473	-11138.60	128.09	22.5763	27.45 (±1.345)

and  $d_s$  is the distance of two outermost carbon atoms when the strain is applied. Strain energy ( $U$ ) is defined as  $E_s - E_0$ , where  $E_s$  is the total energy of the deformed system, and  $E_0$  is the total energy of the undeformed system. Point load is applied to H<sub>2</sub>O(n)@C60 as follows: (a) The structure is relaxed for calculation of the initial total energy of the system. (b) Tensile or compressive strain is applied on two outermost carbon atoms on H<sub>2</sub>O(n)@C60. (c) The two strained atoms are fixed, and other C60 atoms and water molecules inside C60 are relaxed. (d) The strain energy of the deformed system is computed. (e) Steps (b)–(d) are repeated until fracture of the system. Valentini *et al.* applied compression on silicon (Si) nanosphere using plates attached at both ends and showed that the applied load is distributed on the surface of the ball.<sup>23</sup> We also performed MD simulations to apply compression using two plates and compared them with the current DFT result obtained using a point load (see Supplementary material).<sup>24</sup>

Since water molecules can have different orientations inside C60, several structural relaxations with randomly oriented water molecules are performed to find energy-minimized structures, and they are used for mechanical deformations. The structural properties of each of the minimized H<sub>2</sub>O(n)@C60 structures, such as C-C bond-length, interaction energy, and internal pressure are shown in Table I. The initial C-C bond-length for C60 shows reasonable agreement with previous results.<sup>25,26</sup> It should be noted that C-C bond-length increases as more water molecules are encapsulated due to the increase of interaction energy between water and C60. The interaction energy between water and C60 is computed as  $E_{\text{Interaction}} = E_{\text{H}_2\text{O}(n)\text{@C60}} - (E_{\text{H}_2\text{O}(n)} + E_{\text{C60}})$ , and the values from the initially relaxed structures are reasonable when compared to published results.<sup>27</sup> This expansion of buckyball can be also explained by the internal pressure increase, which is induced due to encapsulation of water inside buckyball. In a related study, Pupysheva *et al.* showed that the bond-length of C60 can be increased as more hydrogen is filled.<sup>2</sup> DFT and MD simulations were performed to calculate the internal pressure as shown in Table I. MD simulation is only used for comparing the internal pressure with DFT. The internal pressure ( $P_{I,DFT}$ ) using DFT is computed as  $P_{I,DFT} = (\sum_{i=1}^{60} (F_i \cdot R_i)) / (4\pi R^3)$ , where  $F_i$  is the force vector on the  $i$ th carbon atom,  $R_i$  is the radius vector from the center of the buckyball, and  $R$  is the radius of the buckyball.<sup>2</sup> To compute the pressure using MD simulation, we used LAMMPS package.<sup>28</sup> We used the energy minimized structure of C60 taken from

DFT. Nosé-Hoover thermostat is applied to keep the temperature of H<sub>2</sub>O(n)@C60 constant at 300K. The simulation time step is chosen to be 0.1 fs. We employed the force field discussed in previous work.<sup>29</sup> Each simulation was run for 20ns. Then the internal pressure ( $P_{I,MD}$ ) is calculated as  $P_{I,MD} = (Nk_B T) / V - (1/3V) \langle \sum_i \sum_{i>j} r_{ij} \cdot F_{ij} \rangle$ , where,  $N$  is the number of atoms,  $k_B$  is the Boltzmann constant,  $T$  is the temperature,  $V$  is the volume of C60, and  $r_{ij}$  and  $F_{ij}$  are the distance and force between atoms  $i$  and  $j$  in the system, respectively. Both results confirm that adding more water molecules increase the internal pressure as shown in Table I.

First, we applied hydrostatic strain on H<sub>2</sub>O(n)@C60 with tension and compression. The bulk modulus (Figure 1(a)) is obtained from the total energy variation with respect to the applied hydrostatic strain. The small strain region (−0.08 to 0.08 hydrostatic strain) is fitted using a 5th order polynomial. The bulk modulus of C60 is determined to be 742 GPa, and this is in reasonable agreement with the previous results.<sup>6,7</sup> The bulk modulus increases with the number of water molecules in C60, but the enhancement is not significant.

The variation of the strain energy with the applied volumetric strain for different number of water molecules in C60 is shown in Figure 2(a). In general, all structures show similar energy variation for both types of loading. The effect of

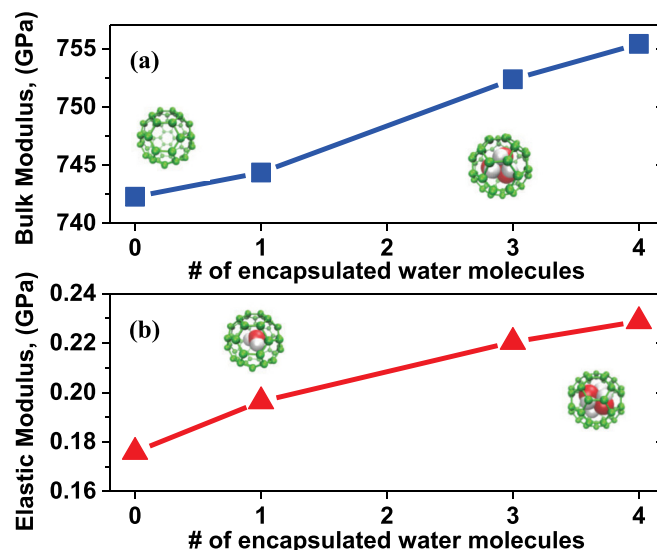


FIG. 1. DFT results for mechanical properties of H<sub>2</sub>O(n)@C60 structures, (a) bulk modulus vs. the number of encapsulated water, and (b) elastic modulus vs. the number of encapsulated water.

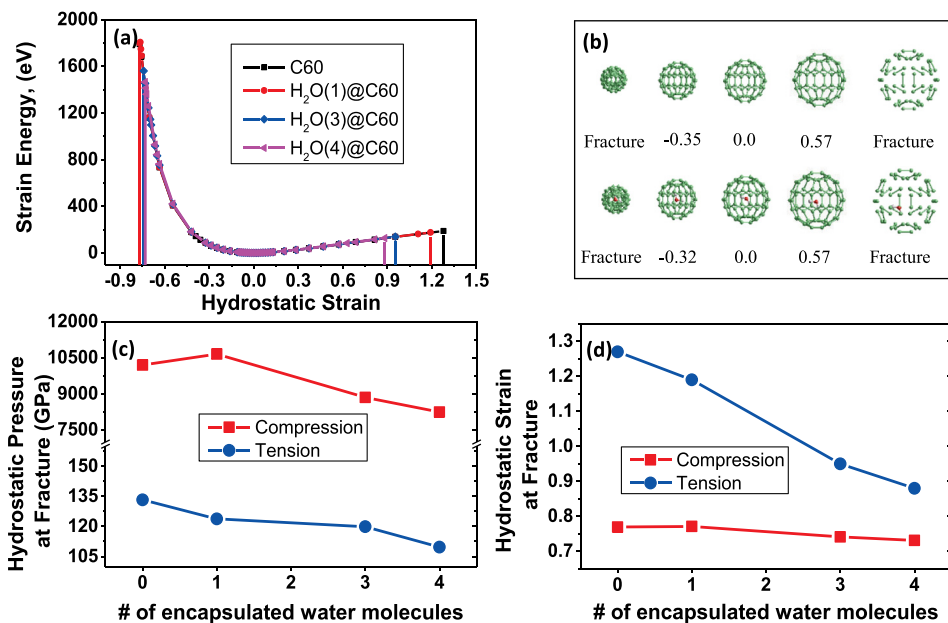


FIG. 2. DFT results for (a) strain energy vs. hydrostatic strain for H<sub>2</sub>O(n)@C60 under hydrostatic compression (negative strain) and tension (positive strain). (b) Molecular structures (C60 (top row) and H<sub>2</sub>O(1)@C60 (bottom row)) at each strain. (c) Hydrostatic pressure at fracture and (d) hydrostatic strain at fracture vs. the number of encapsulated water molecules under hydrostatic compression and tension.

adding water molecules in C60 on the fracture behavior is clearly seen in Figure 2. For hydrostatic tension (HT), both the hydrostatic pressure and hydrostatic strain at fracture of H<sub>2</sub>O(n)@C60 structure decrease as more water molecules are added as shown in Figures 2(c) and 2(d). Since the internal pressure and interaction energy are initially larger for structures with more water, less hydrostatic pressure is required to attain fracture under HT. Failure is initiated when the C-C bond is elongated up to around 1.85 Å. Under hydrostatic compression (HC), it should be noted that the structure can withstand more than ~60 times the pressure at fracture than under HT. Unlike the tension case, the hydrostatic pressure and strain at fracture under compression increase for the 1 water case, but for 3 and 4 waters, they decrease slightly. This is because when the structure is highly compressed up to around fracture, the interaction energy between C60, and water is significantly increased, inducing the structural instability (e.g., at a compressive

strain of 0.70, the interaction energy is 3.38 eV for 1 water, 55.16 eV for 3 waters, and 88.41 eV for 4 waters). This result indicates that the mechanical properties of water-filled (1-water) buckyball can be enhanced, but adding more water does not improve the fracture properties. In addition, it is interesting to note that at the same strain, the structure with more water molecules exhibits higher hydrostatic pressure. This means that one needs to apply more hydrostatic pressure to deform the more water-filled structure up to the same strain. Unlike the tension case, C-C bond dissociation is not observed for HC. In other words, failure of the structure under HC is initiated due to (a) the increased coordination number (from 3 to 5) of the carbon atom, and (b) the interaction between water molecules and H<sub>2</sub>O(n)@C60 wall.

For the point load case, both tension and compression are applied to H<sub>2</sub>O(n)@C60 structures. The mechanical properties are obtained from the strain energy variation with respect to the applied strain as shown in Figure 3(a). First,

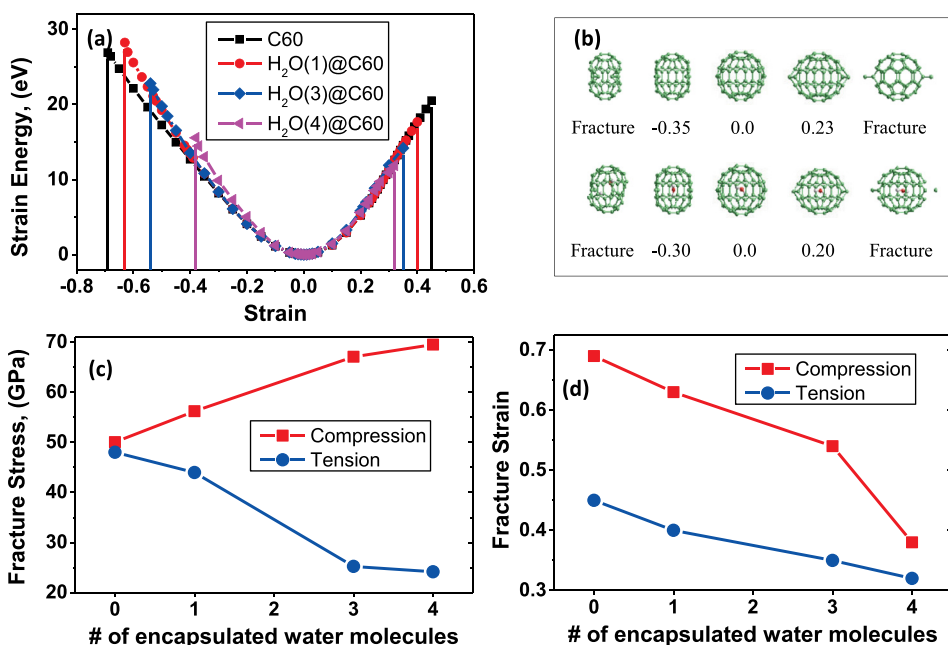


FIG. 3. DFT results for (a) strain energy vs. strain for H<sub>2</sub>O(n)@C60 under compressive (negative strain) and tensile (positive strain) point load. (b) Molecular structures (C60 (top row) and H<sub>2</sub>O(1)@C60 (bottom row)) at each strain. (c) Fracture stress and (d) fracture strain vs. the number of encapsulated water molecules under compressive and tensile point load.

elastic modulus (Figure 1(b)) is computed using the small strain region ( $-0.03$  to  $0.03$  strain), by fitting a 5th order polynomial. As more water molecules are introduced, the elastic modulus increases from 0.18 GPa to 0.23 GPa. The increase is not significant beyond three water molecules in C60.

Under the tensile point load, fracture stress and fracture strain decrease with the increase in the number of water molecules (Figures 3(c) and 3(d)). This behavior is similar to the HT case, which also can be explained by the increased interaction energy (Table I), when more water molecules are added. The fracture of  $H_2O(n)@C60$  is initiated due to the bond-breaking of the C-C bond from regions where the point load is applied. On the other hand, under the compressive point load, the structures with more water can withstand more stress with less fracture strain, as shown in Figures 3(c) and 3(d), which is similar to the case of HC. The applied point load needs to overcome the increased interaction energy, when compressed. When  $H_2O(n)@C60$  is compressed, fracture stresses are comparable (0 and 1-water) or slightly larger (3 and 4-water) than those under tension. When the C60 wall is compressed and becomes closer to the water, carbon and oxygen atoms start to form a covalent bond, which induces the structural instability, and bond dissociation is initiated at the wall after further deformation.

Several interesting observations can be made for  $H_2O(1)@C60$  structure. It has been shown that a single water molecule can rotate freely, meaning that there is no preferable orientation of water.<sup>4,5</sup> Therefore, several tests are performed to verify that mechanical properties are not dependent on the water orientation. For the compression case, the plane of a water molecule is initially placed either perpendicular, horizontal, or at a random orientation to the point load direction. It turns out that in all cases, the plane of the water molecule is positioned perpendicular to the loading direction after about 0.5 compressive strain, and it does not rotate further at a higher strain. In addition, strain energy variations for all the cases are the same. This result confirms that compressive response is independent of the orientation of water. For the fracture behavior, since a water molecule is in the middle of C60 due to the confinement effect, a covalent bond is formed between oxygen and carbon for a strain of 0.6 (bond-length of 1.384 Å, bond-energy of 6.0 eV). The hydrogen in water also forms a bond with the carbon atom (bond-length of 1.032 Å, bond energy of 5.3 eV). However, under tension, a water molecule stays where it was placed with no reorientation because carbon atoms are pulled away from a water molecule, so that the interaction between them is much weaker than in the compression case. For  $H_2O(3,4)@C60$  structures, under compression, the bond between carbon and water is formed around a strain of 0.53 (for 3 waters) and a strain of 0.37 (for 4 waters), which is smaller than in the single water molecule case. This bond formation leads to the failure of the system when further deformation is applied, since it induces the structural instability of C60.

In this Letter, we investigated the effect of encapsulated water molecules inside C60 on its mechanical properties using

DFT calculations. The hydrostatic strain and point load conditions are considered under both tension and compression. The effect of water molecules on the mechanical behavior of C60 is clearly observed in all cases. Under tension, both loading conditions show that the hydrostatic pressure at fracture and fracture stress decrease as more water molecules are added. Under compression, in contrast, structures can withstand more pressure (and stress) at the same strain with more water. This is because, as more water molecules are added in C60, internal pressure and interaction energy between water and C60 increases. Fracture is initiated due to the bond formation between carbon and oxygen atoms under compression and bond-dissociation of carbon under tension. The results shown here suggest that water filled C60s can be good composite agents. Also, mechanical modulation of water filled C60 can be used to form new chemical compounds.

This work was supported by the National Science Foundation under Grant Nos. 0941497 and 1127480.

- <sup>1</sup>K. Kurotobi and Y. Murata, *Science* **333**, 613 (2011).
- <sup>2</sup>O. V. Pupyshcheva, A. A. Farajian, and B. I. Yakobson, *Nano Lett.* **8**, 767 (2008).
- <sup>3</sup>A. Weidinger, M. Waiblinger, B. Pietzak, and T. A. Murphy, *Appl. Phys. A* **66**, 287 (1998).
- <sup>4</sup>B. Ensing, F. Costanzo, and P. L. Silvestrelli, *J. Phys. Chem. A* **116**, 12184 (2012).
- <sup>5</sup>A. B. Farimani, Y. Wu, and N. Aluru, *Phys. Chem. Chem. Phys.* **15**, 17993 (2013).
- <sup>6</sup>R. S. Ruoff and A. L. Ruoff, *Appl. Phys. Lett.* **59**, 1553 (1991).
- <sup>7</sup>J. Cai, R. Bie, X. Tan, and C. Lu, *Physica B* **344**, 99 (2004).
- <sup>8</sup>C. Lee, X. Wei, J. W. Kysar, and J. Hone, *Science* **321**, 385 (2008).
- <sup>9</sup>H. Zhao, K. Min, and N. Aluru, *Nano Lett.* **9**, 3012 (2009).
- <sup>10</sup>K. Min and N. Aluru, *Appl. Phys. Lett.* **98**, 013113 (2011).
- <sup>11</sup>A. Adnan, C. Sun, and H. Mahfuz, *Compos. Sci. Technol.* **67**, 348 (2007).
- <sup>12</sup>Y. Li, *Polymer* **52**, 2310 (2011).
- <sup>13</sup>H. Shen, *Mater. Lett.* **60**, 2050 (2006).
- <sup>14</sup>J. M. Soler, E. Artacho, J. D. Gale, A. García, J. Junquera, P. Ordejón, and D. Sánchez-Portal, *J. Phys.: Condens. Matter* **14**, 2745 (2002).
- <sup>15</sup>T. Dumitrică, T. Belytschko, and B. I. Yakobson, *J. Chem. Phys.* **118**, 9485 (2003).
- <sup>16</sup>P. W. Leu, A. Svizhenko, and K. Cho, *Phys. Rev. B* **77**, 235305 (2008).
- <sup>17</sup>M. Topsakal and S. Ciraci, *Phys. Rev. B* **81**, 024107 (2010).
- <sup>18</sup>W. Ye, K. Min, P. P. Martin, A. A. Rockett, N. Aluru, and J. W. Lyding, *Surf. Sci.* **609**, 145 (2012).
- <sup>19</sup>B. Kumar *et al.*, *Nano Lett.* **13**, 1962 (2013).
- <sup>20</sup>J. P. Perdew, K. Burke, and M. Ernzerhof, *Phys. Rev. Lett.* **77**, 3865 (1996).
- <sup>21</sup>B. Hammer, L. B. Hansen, and J. K. Nørskov, *Phys. Rev. B* **59**, 7413 (1999).
- <sup>22</sup>N. Troullier and J. L. Martins, *Phys. Rev. B* **43**, 1993 (1991).
- <sup>23</sup>P. Valentini, W. Gerberich, and T. Dumitrică, *Phys. Rev. Lett.* **99**, 175701 (2007).
- <sup>24</sup>See supplementary material at <http://dx.doi.org/10.1063/1.4858486> for the comparative study of applying compression using MD and DFT calculations.
- <sup>25</sup>Q. M. Zhang, J.-Y. Yi, and J. Bernholc, *Phys. Rev. Lett.* **66**, 2633 (1991).
- <sup>26</sup>R.-H. Xie, G. W. Bryant, L. Jensen, J. Zhao, and V. H. Smith, Jr., *J. Chem. Phys.* **118**, 8621 (2003).
- <sup>27</sup>C. Ramachandran and N. Sathyamurthy, *Chem. Phys. Lett.* **410**, 348 (2005).
- <sup>28</sup>S. Plimpton, *J. Comput. Phys.* **117**, 1 (1995).
- <sup>29</sup>A. B. Farimani and N. Aluru, *J. Phys. Chem. B* **115**, 12145 (2011).